

LABORATORY DIRECTED RESEARCH AND DEVELOPMENT PROPOSAL
TITLE: GENERATION AND CHARACTERIZATION OF MAGNETIZED BUNCHED ELECTRON BEAM FROM DC PHOTOGUN FOR MEIC COOLER

LEAD SCIENTIST OR ENGINEER:	RIAD SULEIMAN AND MATT POELKER
Phone:	(757) 269-7159
Email:	suleiman@jlab.org
Date:	April 27, 2016
Department/Division:	Center for Injectors and Sources / Accelerator Division
Other Personnel:	
Proposal Term:	From: 10/2015 Through: 10/2018 2nd year If continuation, indicate year (2nd/3rd):

Division Budget Analyst	Kelly Webster
Phone:	(757) 269-7575
Email:	hanifan@jlab.org

This document and the material and data contained herein were developed under the sponsorship of the United States Government. Neither the United States nor the Department of Energy, nor the Thomas Jefferson National Accelerator Facility, nor their employees, makes any warranty, express or implied, or assumes any liability or responsibility for accuracy, completeness or usefulness of any information, apparatus, product or process disclosed, or represents that its use will not infringe privately owned rights. Mention of any product, its manufacturer, or suppliers shall not, nor it is intended to imply approval, disapproval, or fitness for any particular use. A royalty-free, non-exclusive right to use and disseminate same for any purpose whatsoever, is expressly reserved to the United States and the Thomas Jefferson National Accelerator Facility.

Abstract

This LDRD proposal aims to generate magnetized electron beams from a DC high voltage photogun. Simulations and corresponding measurements of beam magnetization as a function of laser pulse dimension and magnetic field strength at the photocathode are planned. Round-to-flat beam transformation will be performed using three skew quadrupoles and the transverse emittance ratios will be measured. Photocathode lifetime at milli-ampere currents will be compared to beam lifetimes with no magnetization, to study the effect of the solenoid field on photocathode ion-back bombardment. Afterwards, a follow-up proposal can be submitted to evaluate the merits of magnetized beam generation using a DC high voltage thermionic gun, with rf-pulsed gridded thermionic emitter.

Combined, these simulations and measurements will benchmark our design tools and provide insights on ways to optimize the MEIC electron cooler, and help us choose the appropriate electron source and injector layout.

1.0 Summary of Proposal

1.1 Description of Project

To achieve the required luminosity, ion beams at MEIC must be cooled. In general, this is accomplished when an electron beam co-propagates with an ion beam moving at the same average velocity ($\langle \gamma_e \rangle = \langle \gamma_i \rangle$), but different temperatures ($T_e \ll T_i$), where the energy of chaotic motion of the ion beam is transferred to the cold electron beam. As proposed by Derbenev [1], the cooling rate can be improved by about two orders of magnitude if the process occurs inside a solenoidal field that forces the electrons to follow small helical trajectories thereby increasing the interaction time with ions and improving the cooling efficiency. This cyclotron motion also provides suppression of electron-ion recombination. Cooling rates with magnetized electron beam are ultimately determined by electron longitudinal energy spread rather than the electron beam transverse emittance as the transverse motion of the electrons is quenched by the magnetic field.

The envisioned MEIC magnetized cooler is part of the Collider ring and aims to counteract emittance degradation induced by intra-beam scattering (IBS), to maintain emittance during collisions and extend the luminosity lifetime. To implement cooling at relatively high energy (electron beam energy 55 MeV ($\gamma=108$)), the electron beam must be bunched and accelerated in an SRF linac. The MEIC cooling solenoid is 30 m long providing a 2 T field. Table 1 summarizes the requirements on the electron beam with noteworthy challenges related to bunch charge and average current, 420 pC and 200 mA, respectively.

Table 1: Requirements on bunched electron beam for MEIC magnetized cooling (at the cooling section).

Bunch length	100 ps (3 cm)
Repetition rate	476 MHz
Bunch charge	420 pC
Peak current	4.2 A
Average current	200 mA
Beam radius at cathode	3 mm
Transverse normalized emittance	10s microns
Solenoid field at cathode	2 kG

One challenge associated with implementing cooling inside the long solenoid of the Collider, is the fringe field immediately upstream of the cooling solenoid. The field lines outside the solenoid magnet introduce very large beam rotation. Derbenev [2] suggested the ill-effects of this fringe field could be cancelled if the electron beam was born in a similar field, but producing beam rotation in the opposite direction, such that the two cancel.

Although, electron cooling with DC electron beams at low energy has been implemented at many labs, no one has yet demonstrated electron cooling with bunched electron beams, or magnetized cooling. Fermi Lab successfully demonstrated non-magnetized relativistic DC cooling at high energy (4.3 MeV) [3]. For Low Energy RHIC Electron Cooling (LEReC) non-magnetized bunched electron beam will be used and eRHIC is planning to use Coherent Electron Cooling (CeC) [4,5].

There are four electron gun options to consider: SRF gun, Normal conducting RF gun (with a photocathode or gridded thermionic cathode), DC high voltage gun (with downstream bunching, or rf-pulsed gridded thermionic emitter), and a DC high voltage photogun.

In general, RF guns are more complicated and expensive compared to DC guns. The biggest challenge for a normal conducting RF gun is thermal heat load management. Typically, normal RF guns are used for pulsed-rf applications. Groups have tried to operate normal conducting RF guns in CW mode but so far, with little success (Los Alamos), or with very low resultant beam energy, comparable to (or lower than) energy produced by DC high voltage photoguns (AES, FarTech). The quarter wave VHF gun developed at LBNL as the source for LCLSII is theoretically on the right track, but so far has had difficulty with field emission from the cathode area. Magnetizing this gun would make this problem worse. SRF guns promise CW operation and with high average current and beam energy, but to date, no effort has come close to achieving the desired high average current (Rosendorf, BNL). Moreover, no attempt has been made to produce magnetized beam from an SRF gun, because the application of a magnetic field on the photocathode is highly problematic to maintaining the superconducting condition of the SRF cavity due to the Meissner effect.

A DC high voltage rf-pulsed gridded thermionic gun, similar to that used at TRIUMF [6], is a viable option since the requirement on gun emittance is not stringent. Of all electron gun options, thermionic guns are considered the closest to “turn-key” technology, relatively simple to operate and maintain, even at very high average current. However, the beam requirements of the Energy Recovery Linac (ERL) may necessitate a smaller emittance from the gun.

Thus we are left with the DC high voltage photogun option. Compared to thermionic guns, photoguns allow for precise control of the electron bunch profile in space and time, which could help to increase the cooling efficiency. Two drawbacks of the dc high voltage photogun are field emission at high bias voltage and the reliance on a relatively delicate photocathode. The JLab gun group has made progress toward minimizing/eliminating field emission. In addition, the gun group has recently manufactured alkali-antimonide photocathodes, shown to be less sensitive to ion bombardment, and demonstrating long lifetime at milli-ampere currents. Based on these considerations, and including our expertise with photoguns, a DC high voltage photogun is the focus of this LDRD proposal.

We also note that a follow-up to this proposal could be submitted to study magnetized beam created using a DC high voltage thermionic gun, with rf-pulsed gridded thermionic emitter. We recently helped TRIUMF develop such a gun, by lending them our original 100 kV thermionic gun. They modified this gun to include the application of rf to the bias grid, and successfully produced rf-bunched beam at high average current and 650 MHz repetition rate, with 100 ps pulses. This gun could be returned to JLab for tests using the same diagnostic beamline and gun solenoid described below.

Examining Table 1, three challenging requirements can be identified. First, the average current is very large. We note that groups from other labs and universities are working hard to achieve high average current and high bunch charge for a variety of applications. The Cornell University group, for example, has recently delivered 65 mA for about 9 hours with lifetime of 2.6 days [7]. Key to this success was the re-discovery of alkali-antimonide photocathode, which is less sensitive to ion bombardment. At JLab, we have used the K_2CsSb photocathode to demonstrate long-lifetime operation at 10 mA average current [8]. The second challenge relates to high bunch charge at high repetition rate. For a DC high voltage gun, this means the gun must be biased at very high voltage, to create a “stiff” beam that is less susceptible to space charge force. We have made relatively good progress developing a 350 kV gun. This work is on-going. The final challenge is the generation and transportation of magnetized bunched electron beam from a gun. Although many labs are pursuing electron cooling, to the best of our knowledge, only one group has been studying *magnetized beam*: the Piot group at the Fermilab Photoinjector Laboratory [9,10]. However, they are not making CW beam at high average current – the new Fermi Lab ASTA injector relies on a pulsed NCRF gun with a Cs_2Te photocathode illuminated by an ultraviolet (UV, $\lambda=263$ nm) laser pulse at 0.5% duty factor [11]. No outside groups appear to be working to develop high average current magnetized beam. This is a very serious problem for the MEIC and the reason we assert the proposed LDRD is essential for JLab.

When discussing magnetized electron cooling, two fundamental topics are involved. The first topic is the interaction between electrons and ions in a longitudinal magnetic field where the presence of a strong field drastically changes the dynamics of the interaction. The second topic is electron beam dynamics in a solenoid magnetic field where the effect of the fringe radial field is accounted for. There are two different motions: one is the helical cyclotron motion in the uniform longitudinal solenoid field due to the transverse velocities of the electrons arising from finite emittance. This motion has a very small radius and a very small resultant emittance. The second rotational motion is due to the azimuthal kick from the fringe radial field at the entrance or exit of a solenoid. This motion has a very large radius (the radius is half of the initial radial displacement of the electron from the solenoid axis) and a very large resultant emittance. For a focusing solenoid, the beam enters and exits the solenoid and the two azimuthal kicks cancel each other. For magnetized electron cooling, the electron beam is being used inside the cooling solenoid (where it suffers an azimuthal kick when it enters). This kick is cancelled by an earlier kick at the exit of the cathode solenoid where the electron beam was born inside it. The narrative of magnetized electron cooling is described below using cylindrical coordinates (r, ϕ, z) with the vector momentum written as: $\vec{p} = p_r \hat{r} + p_\phi \hat{\phi} + p_z \hat{z}$. (Boltzmann constant, $k_B = 8.617 \times 10^{-5}$ eV/K, $m_e c^2 = 510998$ eV, $c = 299792458$ m/s, $e/m_e = 1.759 \times 10^{11}$ rad/(s T)):

1. Electrons are born in a uniform magnetic field $B_{cath} = B_z = 0.2$ T where the electron beam radius is $a_0 = 3.0$ mm (this is the same as the laser spot size). The K_2CsSb photocathode effective temperature is about $T_{eff} = 1000$ K (with 532 nm green laser). For this cathode the transverse thermal energy is $k_B T_{eff} = 0.086$ eV, the transverse momentum is $p_{\perp 0} = \sqrt{2m_e k_B T_{eff}} = 296.8$ eV/c and the thermal emittance is $\epsilon_{th} = a_0 \frac{p_{\perp 0}}{2m_e c} = a_0 \sqrt{\frac{k_B T_{eff}}{2m_e c^2}} = 0.87$ μm .
2. For a gun HV of 350 kV, $\beta = 0.8048$, $\gamma = 1.685$ and the momentum in the z direction is $p_z = \beta \gamma m_e c = 693$ keV/c.
3. Since the electrons are born with transverse thermal momentum in magnetic field, each electron will have a helical cyclotron motion with radius $r_c = \frac{p_{\perp 0}}{eB} = 4.95$ μm . This cyclotron radius is very small when compared to the electron beam radius. The cyclotron frequency is $\omega_c = \frac{eB_z}{\gamma m_e} = 2.09 \times 10^9$ rad/s.
4. The emittance (cyclotron emittance) due to cyclotron motion is: $\epsilon_c = \frac{k_B T_{eff}}{eB_z c} = 0.00144$ μm ; very small when compared to thermal emittance.
5. After traveling a few centimeters from the photocathode, the electrons exit the longitudinal solenoid field but they encounter a returning solenoid radial field which exerts torque on the electrons that produces a rotating trajectory. This beam rotation must be tailored to cancel out similar motion encountered when entering the field of the cooling solenoid.
6. Busch's theorem represents the conservation of canonical angular momentum (CAM) and states that $L = \gamma m_e r^2 \dot{\phi} + \frac{e}{2\pi} \psi$ is a constant, where $\dot{\phi} \equiv \frac{d\phi}{dt}$ is the

angular velocity and $\psi = \int \mathbf{B} \cdot d\mathbf{S}$ is the magnetic flux enclosed by the particle trajectory (i.e., the flux inside a circle with radius r given by the radial distance r of the particle from the z-axis).

7. From Busch's theorem, at the photocathode, $L = \frac{e}{2\pi}\psi$ and $\psi = \int \mathbf{B} \cdot d\mathbf{S} = \pi r^2 B_z$, that is for an electron $L = \frac{1}{2}eB_z r^2$. And after leaving the solenoid $L = \gamma m_e r^2 \dot{\phi}$. For cylindrically symmetric gaussian beam with rms size of a_0 , $\langle r^2 \rangle = 2a_0^2$ and the average canonical angular momentum for the electron beam is $\langle L \rangle = eB_z a_0^2 = 1800$ (neV s) at the photocathode and $\langle L \rangle = 2\gamma m_e a_0^2 \dot{\phi} = 1800$ (neV s) after existing the solenoid.
8. The average angular velocity is $\dot{\phi} = \omega_L = \frac{eB_z}{2\gamma m_e} = 1.04 \times 10^{10}$ rad/s (i.e., the beam rotates at the Larmor frequency, $\omega_L = \frac{\omega_c}{2}$). The average mechanical momentum in the ϕ direction is $p_\phi = \gamma m_e a_0 \dot{\phi} = 89.94$ keV/c. The electron momentum now has a phi component in addition to the axial z-component.
9. The average rotational kinetic energy is $T_\phi = \sqrt{(m_e c^2)^2 + p_\phi^2 c^2} - m_e c^2 = 7854.3$ eV. This is small (2.24%) when compared to the maximum longitudinal kinetic energy of $T_z = 350000$ eV. The total kinetic energy is still $T_z + T_\phi = 350000$ eV (i.e., part of the longitudinal (axial) kinetic energy turns into rotational energy in the phi direction).
10. The electron beam leaves the cathode solenoid field rotating and acquires an angular momentum but once in field-free region where there is no centripetal force, the beam rotates and simultaneously expands as it propagates. As it expands, its angular velocity decreases to conserve angular momentum.
11. The beam size increases as the beam propagates such that the angular momentum of the beam is conserved. Focusing solenoids installed after the exit of the gun and throughout the injector prevent the magnetized beam from blowing up.
12. After leaving the cathode solenoid, and due to beam rotation induced by radial field the *magnetized beam* will have an emittance (called drift or magnetized emittance) of $\epsilon_d = \frac{eB_z a_0^2}{2m_e c} = 528$ μm , or in general, $\epsilon_d [\mu\text{m}] \sim 29.3 [\text{kG}] \sigma_e^2 [\text{mm}]^2$.
13. The cyclotron emittance and drift emittance are related as $\epsilon_{th} = \sqrt{\epsilon_c \epsilon_d}$ where the ratio is $\frac{\epsilon_d}{\epsilon_{th}} = \sqrt{\frac{\epsilon_d}{\epsilon_c}} = \frac{a_0}{r_c} = 606$.
14. The electron beam is accelerated in SRF linac to high energy.
15. The magnetized beam is a coupled beam, and for the kicker section in the circulator-cooler ring, it is easier if the beam is transformed to a flat beam. This can be done with three skew quads (aka, Round-to-Flat Beam (RTFB) Transformer). This transformation produces a beam with very large transverse emittance ratios. For round beam, $\epsilon_x = \epsilon_y$, in contrast to flat beam where $\epsilon_x \gg \epsilon_y$.

16. Bush's theorem states that CAM is preserved in any axisymmetric magnetic field. A quadrupole triplet does not do so; ultimately it can turn CAM to zero (in case when the cyclotron emittance is zero, i.e., practically very small compared with the drift one) and also restore it later when needed.
17. If the beam was transformed to flat in the kicker section, then before entering the cooling solenoid, the beam is transformed back to round beam (magnetized beam) with Flat-to-Round Beam (FTRB) Transformer that restores the initial magnetization.
18. At the entrance of the cooling solenoid, the radial field exerts a torque (opposite to cathode solenoid torque) so the beam is not rotating any more (note that the magnetic field in both solenoids must be in the same direction). This can be achieved when $B_{cath} a_0^2 = B_{cool} \sigma_e^2$, where $B_{cool} = 2.0$ T and electron beam radius in the cooling section is $\sigma_e = 0.95$ mm.
19. Typical radius of the ion beam in the cooling solenoid is 1.0 mm with normalized emittance of about $\epsilon_{ion}^n = 0.4$ μm . The cooling in the Collider ring aims to maintain this low emittance. The effect of the fringe radial field on ions is suppressed by the ratio of the ion mass to the electron mass ($m_p/m_e = 1836$).
20. Once inside the cooling solenoid, the electrons only have a cyclotron motion with radius $r_c = \frac{p_{\perp 0}}{eB} = 0.49$ μm but no rotational motion due to the fringe radial field. The cyclotron emittance due to this motion is $\epsilon_c = \frac{k_B T_{eff}}{eB_{cool} c} = 0.000144$ μm .
21. If the beam is not magnetized from the gun, then the additional rotational motion when it enters the cooling solenoid will make it much hotter than the ion beam ($\epsilon_d = 528$ μm). Instead the emittance will be very close the thermal emittance from the cathode – since the cyclotron emittance is very small (albeit with some degradation due to space charge emittance growth but this can be compensated with focusing solenoids in the beamline).
22. Hence: if the beam is not magnetized from the gun then no cooling can take place in a solenoid. Furthermore, magnetic shielding is now needed in the cooling section; non-magnetized cooling has very strong dependence on relative angles between electrons and ions and strict control of remnant magnetic fields is required to minimize the transverse angular spread in the cooling section.
23. In the cooling solenoid, the electron energy is 55 MeV, with $\beta = 0.999957$ and $\gamma = 107.63$.
24. For magnetized beam in the cooling solenoid, the cyclotron frequency is $\omega_c = \frac{eB_{cool}}{\gamma m_e} = 3.27 \times 10^9$ rad/s, or $f_c = \frac{\omega_c}{2\pi} = 0.52$ GHz. Over the length of the cooling solenoid of 30 m, the electron will finish 52 periods of its cyclotron rotations.
25. The helical motion of the electrons in the magnetic field increases the electron-ion interaction length, thereby significantly improving the cooling efficiency. In particular, electron-ion collisions that occur over many cyclotron oscillations and at distances larger than the cyclotron radius are insensitive to the transverse

velocity of the electrons. This cyclotron motion also provides suppression of electron-ion recombination.

26. In general, electron cooling is preferred at low energy. At higher energies the cooling rate picks up a factor of $1/\gamma^2$ due to Lorentz contraction and time dilation. In the electron-ion rest frame, the length of the cooling solenoid is only $30/\gamma = 0.28$ m. In addition, in their rest frame, the electron and ion stay together for only $30/(\beta c \gamma) = 90/\gamma = 0.84$ ns.
27. Electron-ion collisions are described by Rutherford's scattering formula and is determined (and hence the cooling rate) by the relative particle velocities' spread, $\Delta(\vec{v}_e - \vec{v}_i)$ in the co-moving frame ($\vec{v}_\perp = \gamma c \vec{\theta}$, $\vec{v}_\parallel = c \Delta\gamma/\gamma$), where $\vec{\theta}$ is the transverse angle deviations.
28. For non-magnetized beam, the cooling rate is $\lambda \propto 1/v_{e\perp}^3$ while for magnetized beam, the cooling rate is $\lambda \propto 1/(v - v_{e\parallel})^2$. Electron beam energy spread in MEIC cooler is required to be $\Delta\gamma_e/\gamma_e \leq 10^{-4}$.
29. Cooling solenoid must have high parallelism of magnetic field lines, $\frac{\Delta B_\perp}{B} \approx \sqrt{\frac{\epsilon_{ion}^n}{\beta\gamma\beta_{match}}} \approx 10^{-4}$, where $\epsilon_{ion}^n = 0.4$ μm is the ions normalized emittance and $\beta_{match} = 0.18$ m is the beta function in the cooling solenoid.
30. Upon exiting the cooling solenoid, the beam once again starts rotating due to canonical angular momentum conservation according to Busch's theorem.
31. The spent electron beam enters the Energy Recovery Linac (ERL) and then dumped at low energy.

Figure 1 shows a depiction of the magnetized electron cooling process.

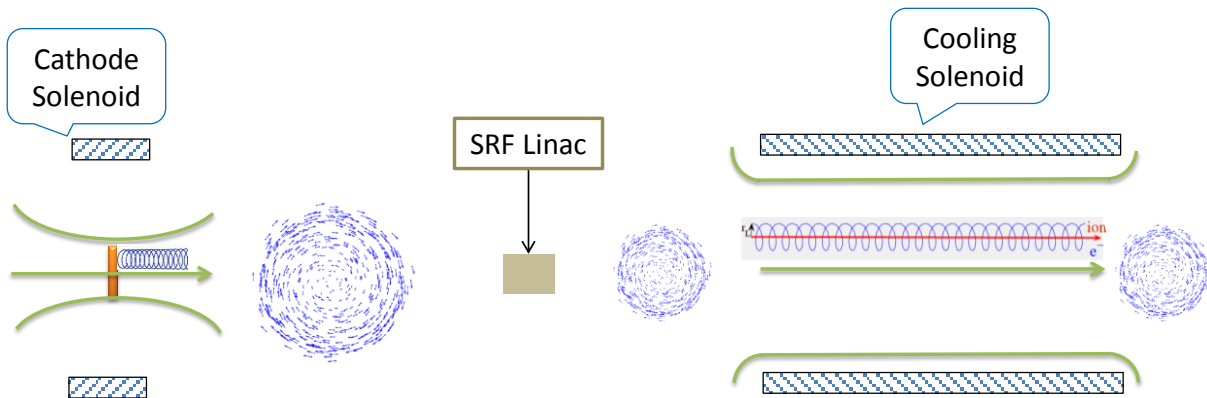


Figure 1: Depiction of magnetized electron beam generation and magnetized cooling in a solenoid.

1.2 Expected Results

- JLab will have direct experience magnetizing a high current electron beam.

- We will learn how the applied magnetic field influences the photocathode lifetime.
- We learn about challenges associated with Round-to-Flat Beam (RTFB) transformations at high bunch charge.
- We will benchmark our simulation tools in this new space-charge dominated, magnetized regime.

2.0 Proposal Narrative

2.1 Purpose/Goals

The goal of this LDRD is to generate a magnetized beam and measure its properties. The impact of the cathode solenoid on the operation of the photogun will be explored. These simulations and measurements will provide insights on ways to optimize the MEIC electron cooler, and help us design the appropriate electron source.

2.2 Approach/Methods

Experimental Overview:

A schematic layout of the experimental beamline is shown in Figure 2. We will use the gun and injector beamline that is being built now at the Gun Test Stand (GTS) to carry out the proposed LDRD work. Some modification to the beamline will be required. Noticeably the addition of skew quadrupoles for the RTFB transform. We will follow the prescription outlined in Ref. [12] to design the three skew quadrupoles. Simulations will be used to determine the appropriate location of the diagnostic crosses.

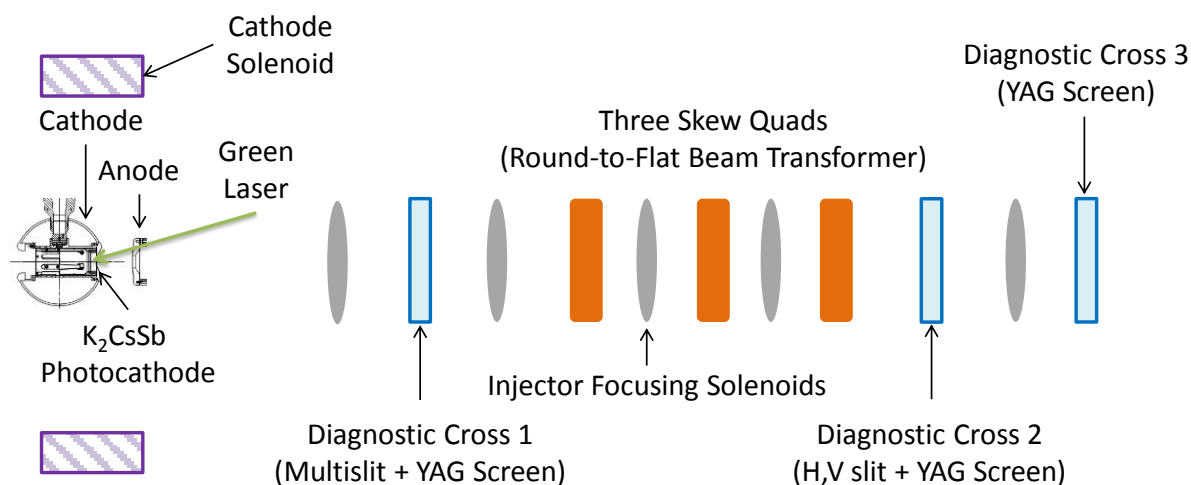


Figure 2: Proposed beamline to generate magnetized beam and measure beam magnetization. Focusing solenoids will be installed between the exit of the gun and dump to prevent the magnetized beam from blowing up.

The gun is an inverted ceramic with a K_2CsSb photocathode and a green 532 nm drive laser (with repetition rates of 4.76 MHz to 476 MHz). We have two HV supplies: Spellman 225 kV and 32 mA and Glassman 550 kV and 5 mA (with SF_6 system). Figure 3 shows the HV chamber. For the proposed LDRD work we need to design and build a solenoid to produce 2 kG at the photocathode with uniformity over the active area to be specified as part of this project.

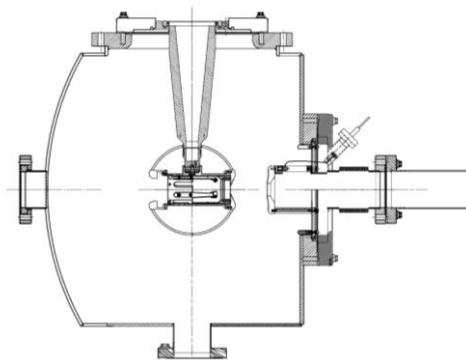


Figure 3: Photogun HV chamber with inverted ceramic and a ball cathode. A solenoid magnet will be installed around the chamber to generate uniform field at photocathode.

Simulation Plan:

The electron beam parameters from the injector required to meet the MEIC cooling specification are unique. Producing low energy, magnetized beam that is space charge dominated has not been previously investigated in depth by the accelerator community. We will use simulation tools to create a physics design for the beamline so we can locate magnets and diagnostics at their optimum positions. Simulation of different operating scenarios of bunch charge, magnetization, bunch shape etc. will be benchmarked against measurements of emittance and other beam parameters (detailed below). As the beams will be space charge dominated, there will be some limit to the aspect ratio that can be achieved with the RTFB transform. Simulation will allow us to quantify how good or complete this can be made for different settings. These results will guide the design of the MEIC injector in the future.

To speed up the benchmarking process, we would ideally like to automate the process of measurement taking and comparison to a virtual machine. This can be achieved using a free Matlab to EPICS interface (as used at SLAC and Cornell University). Matlab scripts can then be used to take measurements and simulate those conditions for comparison, using actual component settings as input.

Measurement Plan:

1. Generate magnetized beam and measure magnetization for different laser spot sizes, ($a_0 = 0.1 - 3$ mm), bunch charges (1 – 500 pC), bunch lengths (50 – 150 ps) and solenoid fields (0 – 2 kG). The magnetization will be measured using Diagnostics Cross 1 and Diagnostic Cross 2 with the three skew quads off via

$$\langle L \rangle = 2p_z \frac{\sigma_1 \sigma_2 \sin \phi}{D} = eB_z a_0^2$$

where σ_1 is the beam radius measured at Diagnostic Cross 1 and σ_2 is the beam radius measured at Diagnostic Cross 2. The drift between the two crosses is D and p_z is the longitudinal momentum of the beam (for a gun HV of 350 kV, $p_z = \beta\gamma m_e = 693 \text{ keV}/c$). The angular rotation ϕ (see Figure 4) is measured from the beam image at Diagnostics Cross 2 when the multislit is inserted at Diagnostics Cross 1. Figure 5 shows an example of a mechanical measurement done at Fermilab.

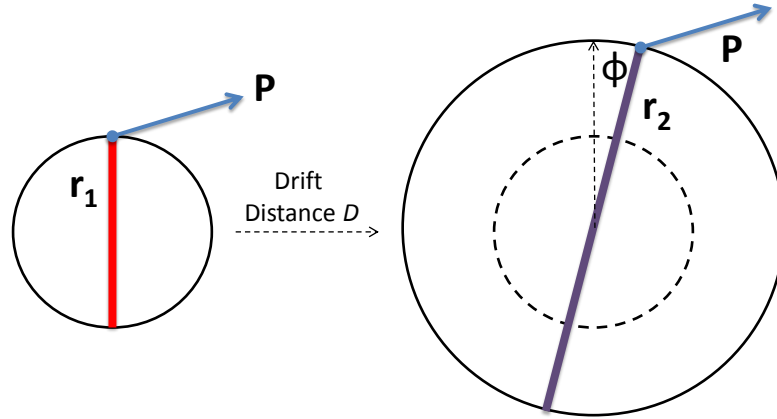


Figure 4: Simultaneous expansion and rotation of a beam with angular momentum in a field-free region.

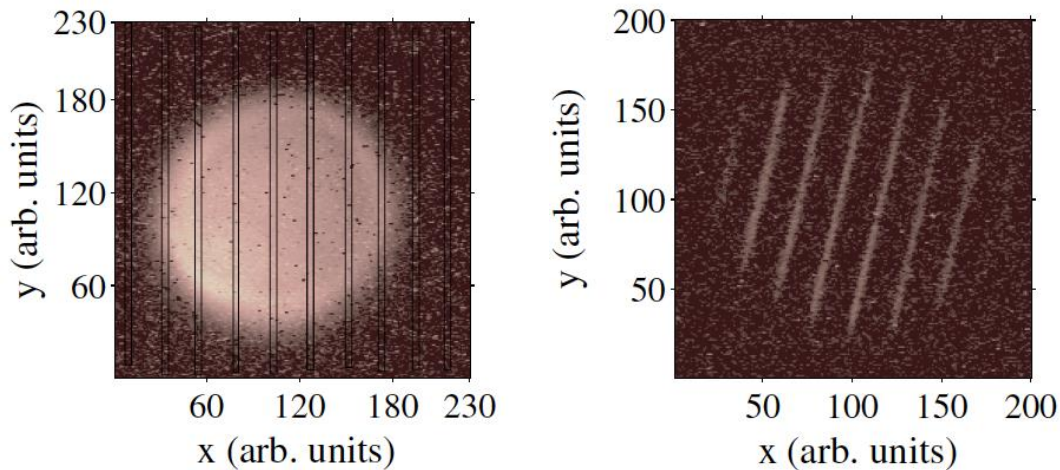


Figure 5: Example of data set used for mechanical angular momentum measurement at Fermilab. Figure from Ref. [9].

2. Use the three skew quads – RTFB Transformer proposed by Derbenev [13] – to generate a flat beam with transverse emittance ratios of $\frac{\epsilon_x^n}{\epsilon_y^n} = \frac{\epsilon_d}{\epsilon_c} = \frac{r_c^2}{a_0^2} \gg 1$.

The horizontal and vertical emittance will be measured using the slit method. Diagnostics Cross 2 will be equipped with a horizontal and vertical slits. The size of the emittance dominated beamlets passed through the slits will be measured, after a drift distance D , with a YAG viewer in Diagnostics Cross 3. Assume that the horizontal beam radius measured at Diagnostics Cross 2 is σ_{2h} and the horizontal radius of the beamlet at Diagnostics Cross 3 is σ_{3h} when a vertical slit is inserted at Diagnostics Cross 2, then the horizontal emittance is $\epsilon_x^n = \gamma\sigma_{2h}\sigma_{3h}/D$. Similarly the vertical emittance can be measured using a horizontal slit.

3. Generate very high currents magnetized beam and study beam transport and RTFB transformation versus electron bunch charge.
4. Measure magnetized photocathode lifetime at high currents (up to 32 mA) and high voltages (200 – 350 kV).
5. Study beam halo and beam loss versus magnetization. We can do that using three different techniques:
 - I. Use ion pumps equipped with very sensitive current readback to monitor vacuum.
 - II. Radiation will also be monitored using x-ray detectors placed around the gun and beamline.
 - III. We will measure the beam intercepted at the floating anode.

2.3 Specific Location of Work

The work will be performed in the FEL Gun Test Stand. Figures 6 and 7 show the existing beamline. This beamline will be modified to install the three skew quadrupoles and a beam dump.

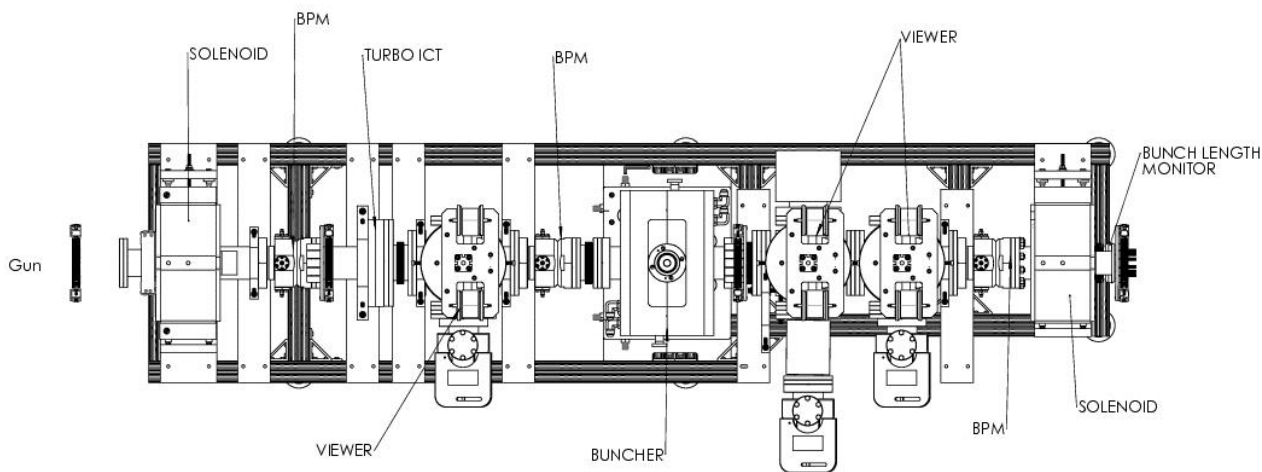


Figure 6: The existing beamline top view. There is no buncher installed; only a drift beamline, where the three skew quads will be installed.

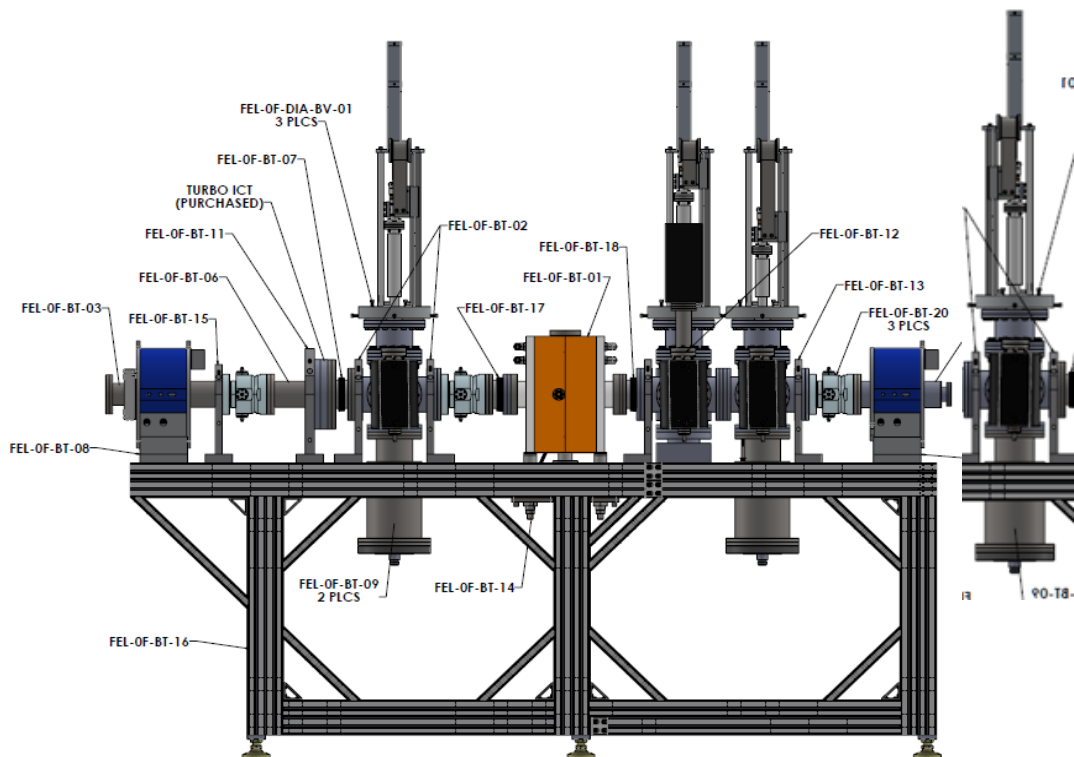


Figure 7: The existing beamline between the gun and the dump. This beamline will be modified to install the three skew quadrupoles. The buncher will not be installed (orange object).

2.4 Anticipated Outcomes/Results

We hope to demonstrate experimentally many aspects of the magnetized bunched electron beam for the MEIC cooler, with the notable exception of 200 mA average beam current. We are limited by the in-house HV supplies to 32 mA.

- Demonstrate ~30 mA magnetized beam at ~220 kV
- Quantify any difference in lifetime of K_2CsSb between magnetized and non-magnetized beam
- Measure magnetization for a variety of charge, bunch dimensions, solenoid strength etc. guided by MEIC specifications.
- Quantify the quality of RTFB transform for a variety of charge, bunch dimensions, solenoid strength etc.
- Demonstrate reliable simulation tools and methods.
- Improve experimental techniques with new machine operation interface.

3.0 Prior Year Accomplishments

3.1 Gun Magnet

Designed magnet and bought it. Will be on site by July 8, 2016.

3.2 Simulations

4.0 VITA (Lead Scientist)

MATTHEW POELKER
Thomas Jefferson National Accelerator Facility
Newport News, VA 23606

Office Phone: (757) 269-7357

Rank: Senior Staff Scientist

e-mail: poelker@jlab.org

DISCIPLINE: Polarized electrons,
Photoelectron guns, Lasers, Vacuum

(a) Professional Preparation

B.S., Engineering Physics, University of Illinois, Champaign/Urbana, IL, December 1983

M.S., Electrical Engineering, Northwestern University, Evanston, IL, June 1988

Ph.D., Electrical Engineering, Northwestern University, Evanston, IL, June 1992

Postdoctoral research associate, Physics Division, Argonne National Lab, January 1992 to May 1994

(b) Appointments

1994-present: Staff Scientist and Group Leader Center for Injectors and Sources,
Thomas Jefferson National Accelerator Facility

(c) Recent Journal Publications

1. "Improving the Performance of Stainless-Steel DC High Voltage Photoelectron Gun Cathode Electrodes via Gas Conditioning with Helium or Krypton." M. BastaniNejad, A. A. Elmustafa, E. Forman, J. Clark, S. Covert, J. Grames, J. Hansknecht, C. Hernandez-Garcia, M. Poelker, R. Suleiman, Nucl. Instr. and Meth. A **762** 135 (2014).
2. "Outgassing Rates of Identical Stainless Steel Chambers Subjected to Different Heat Treatments and with Different Coatings." M. A. Mamun, P. A. Adderley, M. L. Stutzman, M. Poelker and A. A. Elmustafa, Journal of Vacuum Science and Technology A **32**, 021604 (2014).
3. "Measurement of Electron Beam Polarization from Unstrained GaAs via Two-Photon Photoemission." J. L. McCarter, A. Afanasev, T. J. Gay, J. Hansknecht, A. Kechiantz, M. Poelker, Nucl. Instr. and Meth. A **738**, 149 (2014).
4. "A search for spin-polarized photoemission from GaAs using light with orbital angular momentum." N. B. Clayburn, J. L. McCarter, J. M. Dreiling, M. Poelker, D. M. Ryan, T. J. Gay, Phys. Rev. B **87**, 035204 (2013).

(d) Awards

1. E. O. Lawrence Award Recipient, 2011

(e) Committees

1. International Spin Physics Committee since 2012

RIAD SULEIMAN
Jefferson Laboratory, Suite 8
600 Kelvin Dr., Newport News, Virginia 23606
Work: (757) 269-7159
e-mail: suleiman@jlab.org

Employment

- **JEFFERSON LABORATORY:**
March 2012 - present. Staff Scientist III, Accelerator Division.
January 2007 - February 2012. Staff Scientist II, Accelerator Division.
- **VIRGINIA POLYTECHNIC INSTITUTE AND STATE UNIVERSITY:**
August 2005 - January 2007. Research Scientist.
August 2004 - July 2005. Postdoctoral Research Associate.
- **MASSACHUSETTS INSTITUTE OF TECHNOLOGY:**
July 2002 - July 2004. Senior Postdoctoral Research Associate at the Laboratory for Nuclear Science.
October 1999 - June 2002. Postdoctoral Research Associate at the Laboratory for Nuclear Science.

Education

- **KENT STATE UNIVERSITY:** September 1993 - October 1999.
Ph.D. student at the Center for Nuclear Research of the Physics Department.
Doctor of Philosophy degree in Physics awarded in December 1999.
Thesis project (Adviser: Professor Makis Petratos):
“Measurement of the Electric and Magnetic Elastic Structure Functions of the Deuteron at Large Momentum Transfers”.
- **YARMOUK UNIVERSITY, JORDAN:** February 1990 - May 1993.
Bachelor of Science degree in Physics, 1993.

Professional Affiliation

- American Physical Society

Recent Journal Publications

1. “Measurement of parity violation in electron-quark scattering.” D. Wang et al., *Nature* **506**, **67** (2014).
2. “Charge Lifetime Measurements at High Average Current Using a K_2CsSb Photocathode inside a DC High Voltage Photogun.” R. Mammei, R. Suleiman, et al., *Phys. Rev. ST Accel. Beams*, **16**, 033401 (2013).
3. “First Determination of the Weak Charge of the Proton.” D. Androic et al., *Phys. Rev. Lett.* **111**, 141803 (2013).

5.0 Budget Explanation

To be able to perform the proposed measurements, budget is required for the following procurements:

1. Purchase solenoid magnet to provide 2 kG at cathode
2. Three skew quadrupoles to be used as a round-to-flat beam transformer
3. Components installed inside three diagnostics crosses
4. Beamline hardware: stepper motor controlled bellows, for the multislit and movable single slits for emittance measurements. (note, we have the big ticket items in-house: gun, K_2CsSb deposition chamber, valves, dump, ion pumps, differential pump can and NEG modules, we have 80/20 aluminum support structure)
5. Laser components
6. postdoc

Work performed outside the gun group will need to be paid for with additional budget:

1. Gun magnet design
2. Gun magnet installation
3. Relocate new CEBAF dogleg power supply and provide 480VAC and LCW
4. Mechanical designer for beamline (Gary Hays)
5. Mechanical designer for the slits (Gary Hays)
6. ASTRA and GPT modeling (Fay Hannon)

The grand total cost for the first year is \$339,211 (with overhead). For the gun magnet power supply, we will use new CEBAF dogleg magnet supply (500 A/80 V). For the second year, the grand total cost is \$265,850 (with overhead). For the third year, the grand total cost is \$212,025 (with overhead).

References

1. "Magnetization effects in electron cooling." Ya. Derbenev and A. Skrinsky, *Fiz. Plazmy* **4**, 492 (1978) [*Sov. J. Plasma Phys.* **4**, 273 (1978)].
2. "A low emittance, flat-beam electron source for linear colliders." R. Brinkmann, Y. Derbenev, and K. Flöttmann, *Phys. Rev. ST Accel. Beams* **4**, 053501 (2001).
3. "Experimental Demonstration of Relativistic Electron Cooling." S. Nagaitsev et al., *Phys. Rev. Lett.* **96**, 044801 (2006).
4. "Cooling of High-Energy Hadron Beams." M. Blaskiewicz, *Annual Review of Nuclear and Particle Science* **64**, 299 (2014).
5. "High-energy electron cooling in a collider." A. V. Fedotov et al., *New J. Phys.* **8**, 283 (2006).
6. "The TRIUMF-ARIEL RF Modulated Thermionic Electron Source." F. Ames, *Proc. Of EIC'14*, Newport News, VA (2014).
7. "Record high-average current from a high-brightness Photoinjector." B. Dunham et al., *Appl. Phys. Lett.* **102**, 034105 (2013).
8. "Charge Lifetime Measurements at High Average Current Using a K_2CsSb Photocathode inside a DC High Voltage Photogun." R. Mammei et al., *Phys. Rev. ST Accel. Beams* **16**, 033401 (2013).
9. "Generation of angular-momentum-dominated electron beams from a Photoinjector." Y.-E Sun et al., *Phys. Rev. ST Accel. Beams* **7**, 123501 (2004).
10. "Photoinjector generation of a flat electron beam with transverse emittance ratio of 100." P. Piot et al., *Phys. Rev. ST Accel. Beams* **9**, 031001 (2006).
11. "The Advanced Superconducting Test Accelerator (ASTA) at Fermilab: A User-Driven Facility Dedicated to Accelerator Science & Technology." P. Piot et al., arXiv:1304.0311 [physics.acc-ph] (2013).
12. "Simple algorithm for designing skew-quadrupole cooling configurations." B. Carlsten and K. Bishofberger, *New J. Phys.* **8** 286 (2006).
13. "Adapting Optics for High Energy Electron Cooling." Ya. Derbenev, University of Michigan Report No. UM-HE-98-04 (1998).

Attachments

